In Situ Analysis of the Facets of Cu-Based Electrocatalysts in Alkaline Media Using Pb Underpotential Deposition

Hochfilzer, Degenhart; Tiwari, Aarti; Clark, Ezra L.; Bjørnlund, Anton Simon; Maagaard, Thomas; Horch, Sebastian; Seger, Brian; Chorkendorff, Ib; Kibsgaard, Jakob

Published in:
Langmuir

Link to article, DOI:
10.1021/acs.langmuir.1c02830

Publication date:
2022

Document Version
Publisher's PDF, also known as Version of record

LANGMUIR

pubs.acs.org/Langmuir Article

In Situ Analysis of the Facets of Cu-Based Electrocatalysts in Alkaline Media Using Pb Underpotential Deposition

Degenhart Hochfilzer, Aarti Tiwari, Ezra L. Clark, Anton Simon Bjørnlund, Thomas Maagaard, Sebastian Horch, Brian Seger, Ib Chorkendorff, and Jakob Kibsgaard*

Cite This: *Langmuir* 2022, 38, 1514–1521 Read Online

ACCESS | Metrics & More | Article Recommendations | Supporting Information

ABSTRACT: Establishing relationships between the surface atomic structure and activity of Cu-based electrocatalysts for CO_2 and CO reduction is hindered by probable surface restructuring under working conditions. Insights into these structural evolutions are scarce as techniques for monitoring the surface facets in conventional experimental designs are lacking. To directly correlate surface reconstructions to changes in selectivity or activity, the development of surface-sensitive, electrochemical probes is highly desirable. Here, we report the underpotential deposition of lead over three low index Cu single crystals in alkaline media, the preferred electrolyte for CO reduction studies. We find that underpotential deposition of Pb onto these facets occurs at distinct potentials, and we use these benchmarks to probe the predominant facet of polycrystalline Cu electrodes *in situ*. Finally, we demonstrate that Cu and Pb form an irreversible surface alloy during underpotential deposition, which limits this method to investigating the surface atomic structure after reaction.

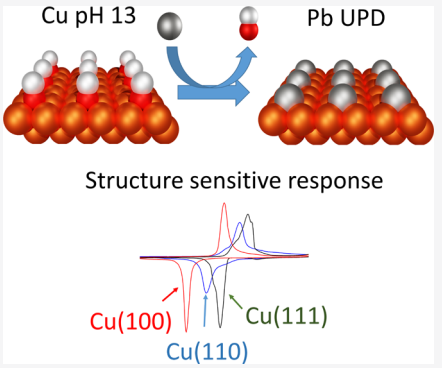

INTRODUCTION

Copper (Cu) has been intensively investigated as an electrocatalyst for various reactions including nitrate, carbon dioxide (CO_2), and carbon monoxide (CO) reduction.[1−3] Electrochemical CO_2 and CO reduction have attracted significant attention as a potential approach for the sustainable production of chemical feedstocks, such as ethylene and ethanol.[4,5] Following the pioneering work from Hori et al., significant efforts have been devoted to elucidating the properties of Cu that enable it to catalyze the reduction of CO_2 and CO into high value hydrocarbons and oxygenated products at relevant rates.[6] Thereby, significant advancements have been made in improving the performance of Cu-based catalysts. However, to date, there is no consensus in the literature on the reaction pathway, active sites, and rate-determining steps toward the various reduction products.[7−13]

A key factor contributing to this discrepancy is most likely the high mobility of Cu under reaction conditions, which leads to morphological changes and restructuring of the catalyst surface and thereby to a potential change of active sites over time. Such restructuring processes are primarily investigated *in situ* by scanning tunneling microscopy (STM) or grazing incidence X-ray diffraction (GIXRD) at synchrotron facilities.[14,15] While these measurements provided indications of possible restructuring processes, they are biased with respect to the scanned location on the catalyst (for STM) or with respect to the set of lattice planes being probed (for GIXRD). Additionally, these measurements cannot easily be combined with analytical techniques for product analysis, which hinders a direct correlation between the surface facet distribution and either activity or selectivity. It is therefore tempting to study morphological changes of the catalyst surface *ex situ* after the reaction. However, this approach carries a significant pitfall as Cu catalysts are intrinsically unstable at open circuit potential, and possible changes in the catalyst morphology during cell disassembly can therefore not be excluded.[16] Additionally, Cu oxidizes rapidly when exposed to air, which possibly also leads to restructuring of the catalyst.

It is therefore highly desirable to develop electrochemical probes that are surface sensitive and can probe changes in the surface atomic structure *in situ* without exposure to air. For CO reduction under alkaline conditions recent approaches have focused on the hydroxide adsorption and desorption features on Cu catalysts or the hydroxide mediated surface oxidation of Cu.[17,18] While these features in the so-called fingerprint region can give insight into the surface atomic structure, there are Cu catalysts without pronounced features in this region.[19,20] Additionally, the probed potential range is dominated by CO oxidation in CO saturated electrolytes, masking the usually investigated features.[21] This motivates the development of more universal electrochemical probes.

Received: October 24, 2021
Revised: January 5, 2022
Published: January 19, 2022

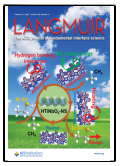

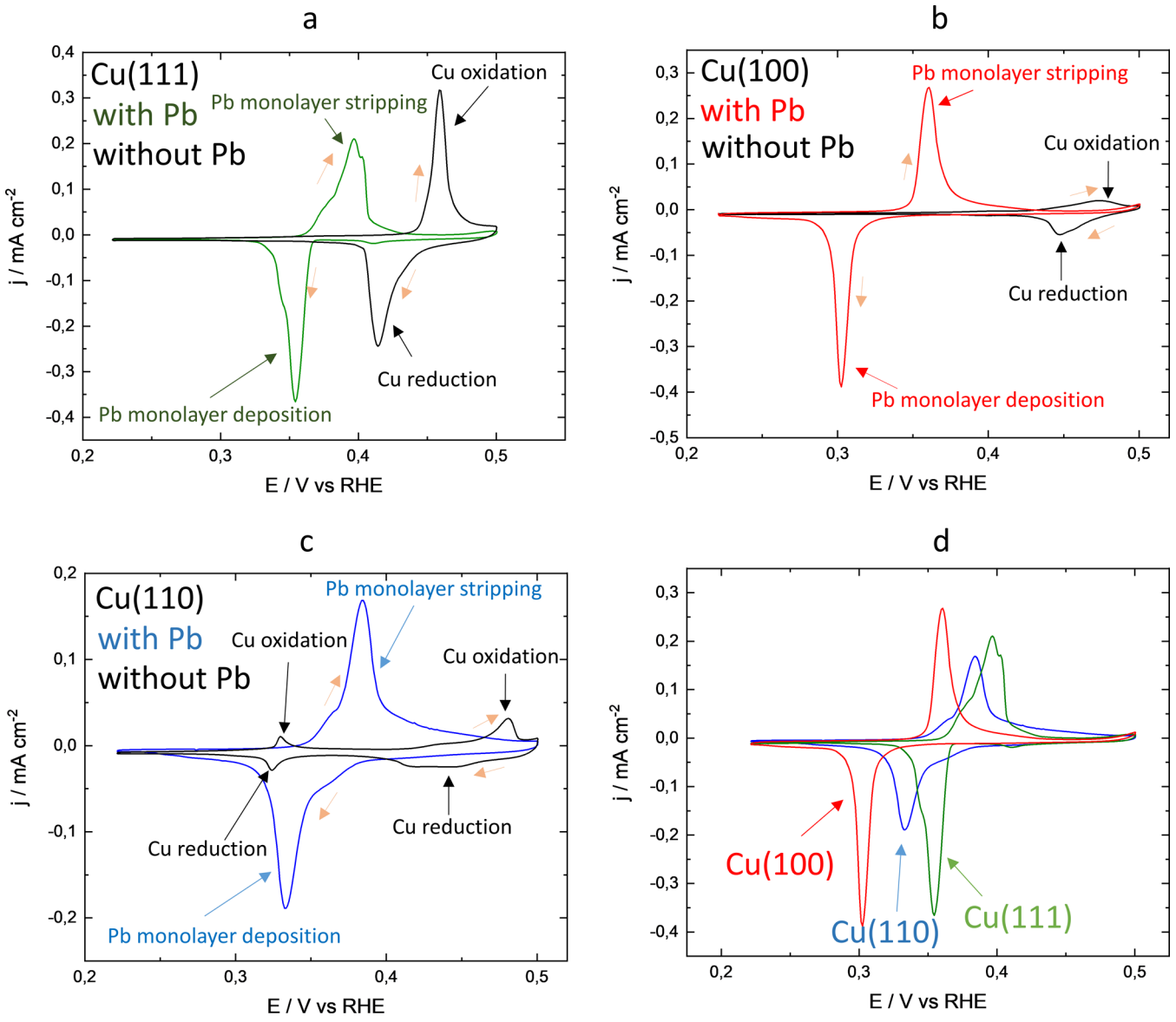

Figure 1. Cyclic voltammograms in 0.1 M KOH and 0.1 M KOH + 1 mM $Pb(NO_3)_2$ at 10 mV/s of (a) Cu(111), (b) Cu(100), and (c) Cu(110). (d) Overlaid Pb-UPD responses of Cu(111), Cu(100), and Cu(110). Orange arrows indicate the scan direction.

A potential candidate is underpotential deposition (UPD), which is a self-limiting process that allows for a controlled electrochemical deposition of a (sub)monolayer of a metal on another metal. This is a well-established electrochemical method that has been used to synthesize catalyst overlayers, poison specific surface sites or determine the surface area of a catalyst.[22−24] In general, the process enables the deposition of metals with a lower work function on to metals with a higher work function, which offers various material combinations that have been explored in the literature.[25,26] The method's dependence on the work function of the substrate also makes the process sensitive to the surface atomic structure of the substrate as different crystal facets have different work functions. This sensitivity results in defined UPD shifts for the respective crystal orientations. An expected UPD shift (ΔU_P), which has been defined as the difference between multilayer stripping and the stripping of the UPD monolayer, can be calculated according to eq 1.[25]

$$\Delta U_P = \alpha \Delta\varphi \quad \text{with } \alpha = 0.5\ \text{V/eV} \tag{1}$$

Here, $\Delta\varphi$ is the difference in work function between the substrate and the adlayer and α is an empirically determined correlation parameter.[25] This has been utilized in the literature to study the surface atomic structure of noble metals such as Au or Pt under acidic and basic conditions.[27] However, despite the significant influence of the surface atomic structure of Cu on its CO reduction activity and selectivity, a similar approach has not been taken to investigate Cu surfaces under alkaline conditions. Only during the preparation of this work has there been a study reporting on the electrochemical characterization of Cu catalysts with Pb-UPD in acidic, halide-containing solutions.[28] This study electrochemically probed the surface atomic structure of polycrystalline Cu electrodes; however, the work is limited to acidic electrolytes. Thereby, a direct application of the method after experiments in alkaline environments, the preferred conditions for electrochemical CO reduction, is hindered. In the course of the necessary electrolyte exchange, the catalyst easily oxidizes in air and needs to be rereduced in the new electrolyte prior to Pb-UPD.

https://doi.org/10.1021/acs.langmuir.1c02830
Langmuir 2022, 38, 1514−1521

This does not only limit the advantages over alternative *ex situ* surface analysis techniques but also carries a significant pitfall as a recent study showed that surface restructuring can originate from oxidation and reduction cycles.[29] Furthermore, the approach requires the presence of halides to obtain well-defined UPD features, which have been shown to alter the surface morphology of Cu.[30] Additionally, investigations of the surface composition after UPD are necessary to evaluate whether Pb-UPD can be performed before and after the reaction on the same Cu sample.

To address these gaps, we present in this paper Pb-UPD experiments in 0.1 M KOH on Cu(111), Cu(100), and Cu(110) and utilize these benchmark cyclic voltammograms (CVs) to electrochemically probe the surface atomic structure of polycrystalline Cu stubs and a sputtered Cu thin film in alkaline conditions. The measurements on single crystal electrodes additionally allow us to show that sharp Pb underpotential deposition on Cu is not fundamentally linked to chloride but an effect of specifically adsorbed anions in general. Furthermore, we show by X-ray photoelectron spectroscopy (XPS) and low energy ion spectroscopy (LEIS) that Pb forms an irreversible surface alloy with Cu upon UPD, which is in agreement with an earlier STM investigation.[31] Thus, low amounts of Pb in Cu are even detectable after the UPD strip is completed, which entails this method is best suited for postreaction monitoring of the surface atomic structure, whereas prereaction monitoring would entail a Pb-contaminated Cu.

EXPERIMENTAL SECTION

Electrochemical Measurements. All electrochemical measurements were performed in a PTFE cell with a reversible hydrogen or Hg/Hg_2SO_4 reference electrode, which was calibrated vs the reversible hydrogen electrode before each experiment. As a counter electrode, a Au wire or a graphite rod was used. The electrolyte was in all cases 0.1 M KOH (Merck, purity 99.995%), which was prepared in a PFA flask.

The Cu(111), Cu(110), and Cu(100) single crystals were obtained from Mateck with a purity of 99.9999%. Following our previous work, the Cu single crystals were prepared by electropolishing in 66% phosphoric acid (prepared from 85% EMSURE, Merck) for 1 min at 2 V vs RHE, and CVs were recorded in 0.1 M KOH in the fingerprint region of the respective single crystals to ensure that the surface is well ordered (Figure S1a–c).[21] Subsequently, Pb was added from a 0.1 M $Pb(NO_3)_2$ stock solution (Sigma-Aldrich, purity 99.999%) during a constant potential hold at 0.4 V vs RHE.

The electrochemical CO reduction experiment was performed with a rotating disk electrode at a rotation rate of 1600 rpm to avoid bubble formation. Additionally, a carbonyl filter was used to purify the CO from transition metal carbonyls.[32]

After each Pb-UPD experiment the PTFE cell was cleaned in aqua regia overnight, washed several times with Milli-Q water, and subsequently stored in an oven at 100 °C for several hours to remove aqua regia residues from the porous PTFE polymer.

The Cu stubs were cut from a Cu rod (Mateck, purity 99.9999%) and subsequently electropolished in 66% H_3PO_4 (85% EMSURE, Merck) at 2 V vs Cu for 2 min or mechanically polished with SiC abrasive paper (CarbiMet, P1200).

The electropolishing step also removed the incorporated Pb in the Cu electrodes after Pb-UPD to have a Pb-free Cu electrode at the start of each experiment.

The Cu thin film was sputter-deposited from a Cu target (AJA International, purity 99.995%) in a commercial sputter chamber (AJA International) with a growth rate of 1 Å/s on glassy carbon stubs (SIGRADUR) for electrochemical experiments and on a Si(100) wafer (Silicon Materials) for XRD characterization. For the glassy carbon samples additionally a 5 nm Ti adhesion layer was deposited.

X-ray Diffraction. Symmetric X-ray diffraction experiments were performed by using a PAN-analytical Empyrian diffractometer with Cu Kα radiation (λ = 1.54178 Å).

X-ray Photoelectron Spectroscopy and Low Energy Ion Scattering. X-ray photoelectron spectroscopy (XPS) was performed on a ThermoScientific Thetaprobe spectroscope with a monochromatic Al Kα source. Survey scans were performed with a pass energy of 200 eV, a step size of 1 eV, and a dwell time of 50 ms. Additionally, scans in the region of Cu 2p and Pb 4f were performed at a step size of 0.1 eV. The data analysis was performed with the Thermo Avantage software.

Ion scattering spectroscopy was performed with the same setup in CRR mode at a He pressure of 2×10^{-7} mbar. The instrument settings were a retardation ratio of 2.5 with a step size of 1 eV and a dwell time of 50 ms with an ion gun set to 1 keV.

RESULTS AND DISCUSSION

Figures 1a–c show the steady-state CVs for Pb-UPD for the three low index Cu(*hkl*) single crystals and the respective CVs in the same potential range without Pb in solution.

The potential limits have been chosen to completely strip the Pb monolayer on the anodic end and to avoid significant bulk Pb deposition on the cathodic end. In this potential range, each facet shows a sharp and distinct monolayer deposition of Pb (in the cathodic going scan) according to eq 2

$$HPbO_2^- + 2e^- + H_2O \rightarrow Pb + 3OH^- \quad (E^0 = -0.540\ \text{V for multilayer deposition}) \tag{2}$$

and stripping (in the anodic going scan) as expected based on their different work functions (Table 1). As predicted by eq 1,

Table 1. Measured and Expected Values for the Underpotential Shift[a]

	ΔU_p^{Meas} (V)	ΔU_p^{Exp} (V)	Q_{UPD} (mC cm^{-2})	Q_{OH} (mC cm^{-2})	$Q_{UPD} - Q_{OH}$ (mC cm^{-2})
Cu(100)	0.133	0.244	0.49	0.058	0.43
Cu(111)	0.169	0.366	0.54	0.078	0.46
Cu(110)	0.157	0.229	0.49	0.025	0.46

[a]The expected value was calculated based on eq 1 while the experimental value was evaluated by using the main UPD stripping peak on the respective single crystals and the reversible potential of eq 2. Measured charge for the UPD of Pb on Cu and OH desorption charge. Work functions for the calculation of the expected UPD shift and OH adsorption charges are taken from ref 17.

the Cu(111) surface has the largest UPD shift of 0.169 V. In line with the lower work function of Cu(100) and Cu(110), which has been shown to most likely reconstruct to Cu(110)-(1 × 2) in the studied potential range, Pb-UPD occurs at more cathodic potentials on these single crystals (Figures 1b,c and Table 1).[17] However, while the calculation suggests the smallest UPD shift on Cu(110)-(1 × 2), we found experimentally the smallest UPD shift on Cu(100) instead. Furthermore, the reversible potentials for Pb-UPD on all single crystals are significantly more cathodic than predicted.

While some uncertainty arises from the spread of reported work functions for the Cu single crystals in the literature, this spread is not sufficient to explain our observation.[33] We rather reason our experimental trend by the influence of hydroxide ions, which are specifically adsorbed on all single crystals prior to Pb-UPD. By correlating the difference between the expected

https://doi.org/10.1021/acs.langmuir.1c02830
Langmuir 2022, 38, 1514–1521

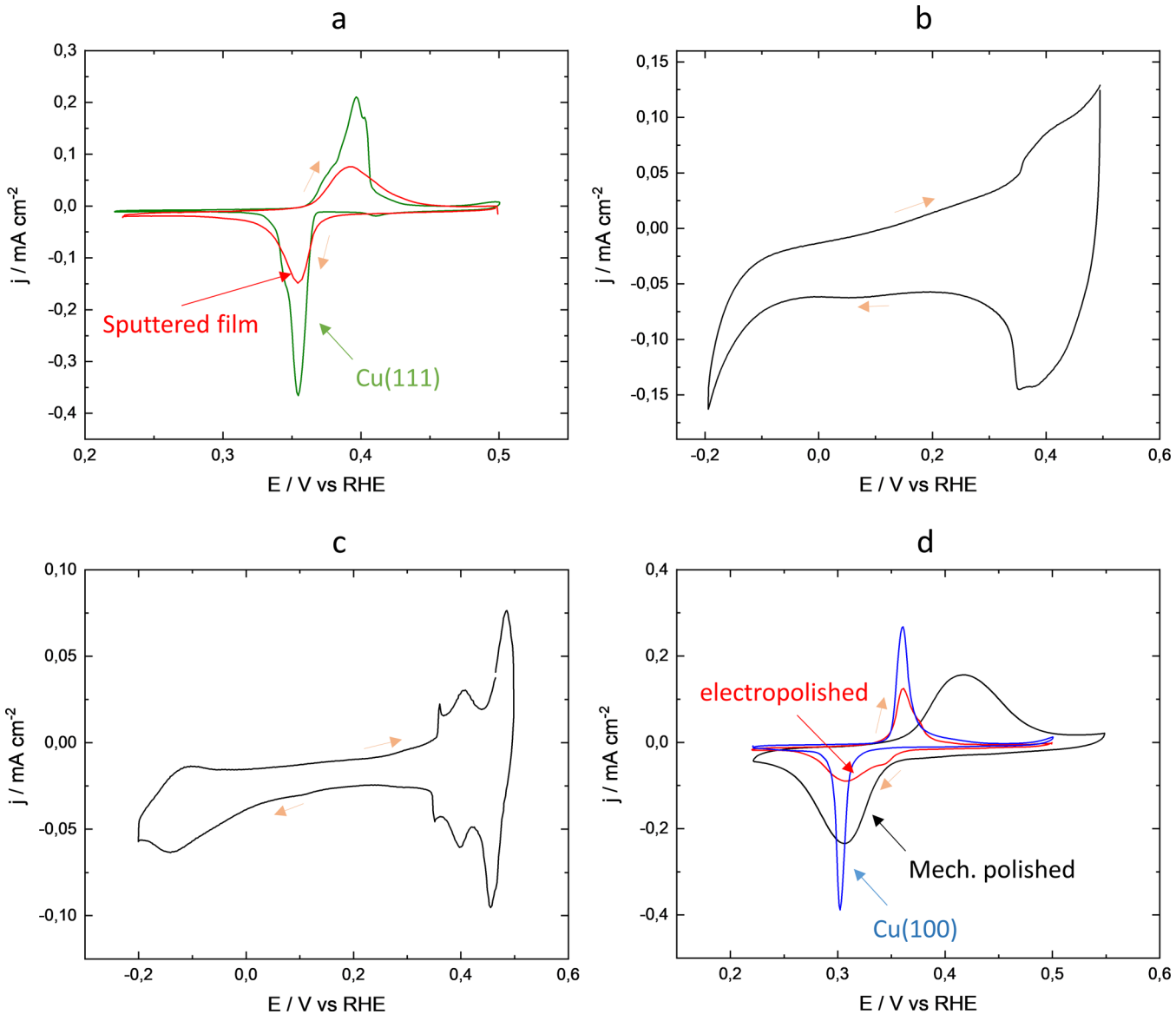

Figure 2. (a) Pb-UPD on a sputtered Cu thin film and Cu(111) at 10 mV/s. (b) Fingerprint CV of a mechanically polished Cu stub at 50 mV/s. (c) Fingerprint CV of an electropolished Cu stub at 50 mV/s. (d) Pb-UPD on the electrochemically as well as mechanically polished Cu stub and Cu(100) at 10 mV/s. Orange arrows indicate the scan direction.

UPD shift and the measured UPD shift with the amount of specifically adsorbed hydroxide anions, it is evident that a larger OH coverage results in a larger deviation from the expected value (Figure S2). As Cu(100) has a significantly higher OH coverage prior to Pb-UPD compared to Cu(110)-(1 × 2), the shift toward more cathodic potentials is more pronounced and results in Pb monolayer deposition at the most negative potential on the Cu(100) surface. The influence of specifically adsorbed anions on the UPD process has been reasoned in the past by a partial electron transfer between the anion and the surface, which reduces the effective work function of the metal.[25] This reduces the difference in work functions between the substrate and the UPD adlayer, resulting in a shift of the UPD peak to more negative potentials such as predicted by eq 1. Alternatively, a decline in the UPD shift has been also reasoned by the formation of a 2D adlayer of the specifically adsorbed ion on the metal substrate (in our case $(CuOH)_{2D}$).[34,35] The UPD then proceeds by the replacement of the OH adlayer with a Pb adlayer, which results in a negative shift of the UPD peaks compared to the deposition on the metallic substrate. Additionally, the OH desorption charge also has to be considered when calculating the Pb-UPD charge as OH has to be displaced to deposit Pb (Table 1).

In comparison to the Pb deposition peaks, the monolayer stripping peaks are less separated on the different single crystals (Figure 1d). This results from a higher reversibility of the UPD process on Cu(111) compared to Cu(100) and Cu(110)-(1 × 2). The higher reversibility of Pb-UPD on Cu(111) is potentially linked to the higher OH coverage on this single crystal. Specifically adsorbed anions have been proposed to improve the reaction kinetics of UPD processes by accelerating the transfer of electrons as a bridging species or by breaking the hydration shell of the metal ion in solution.[35] Alternatively, the difference in reversibility could also be the result of different alloying and dealloying kinetics on the different single crystals as Cu and Pb have been shown to form a surface alloy.[36,37] While this surface alloy has been investigated in detail by surface science methods, little is

https://doi.org/10.1021/acs.langmuir.1c02830
Langmuir 2022, 38, 1514−1521

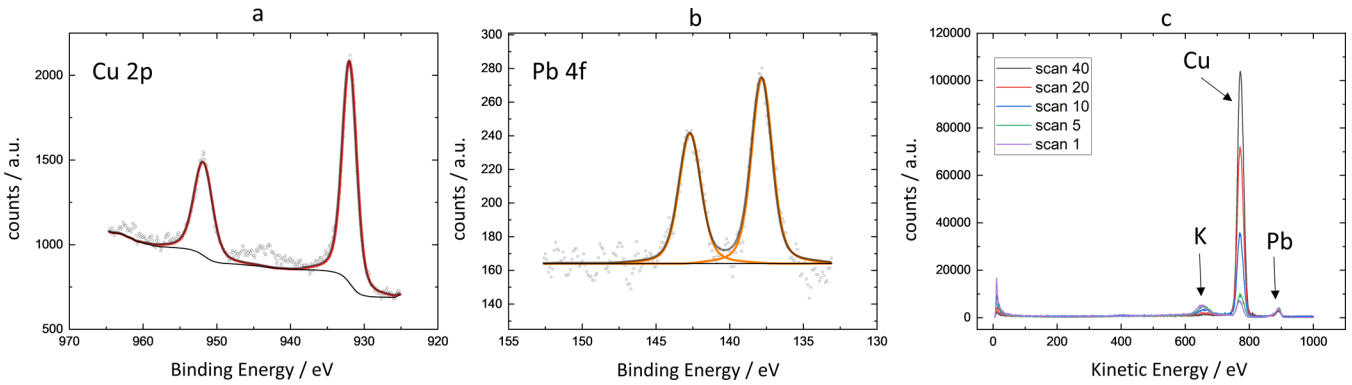

Figure 3. XPS core level scans of Cu 2p (a) and Pb 4f (b) and LEIS scans with 1 keV acceleration voltage (c) of Cu(111). The electrode was polarized to 0.5 V vs RHE prior to breaking contact with the electrolyte.

known about the influence of Pb on the electrochemical characteristics of Cu.[36−39]

With the benchmark CVs on the low index Cu single crystals established, we investigated the Pb-UPD response on polycrystalline Cu electrodes, which are generally used in the literature to study the CO reduction activity of Cu (Figure 2).

We investigated two types of polycrystalline Cu samples, namely, a sputtered thin film and a Cu stub. The sputtered film is expected to have a predominant (111) texture, which is also confirmed by X-ray diffraction and the fingerprint CV (Figures S3 and S4).[40] In line with this characterization, the Pb-UPD response of the sputtered Cu thin film is in good agreement with the Cu(111) single crystal, confirming that Pb-UPD can probe the surface of a polycrystalline material in alkaline conditions (Figure 2a). Building on this successful application of our methodology, we studied the Pb-UPD response of a polycrystalline Cu stub prepared by either electropolishing or mechanical polishing. The electrode prepared by electropolishing shows defined OH adsorption and desorption features that can be ascribed to the presence of Cu(100) (Figure 2c).[20] However, it should be noted that previously a preferential Cu(111) texture on polycrystalline Cu stubs has been reported.[28] The discrepancy in the exposed facets possibly results from a different history of the samples or the exact preparation procedure. This result also highlights the importance of characterizing the exposed facets of polycrystalline samples under working conditions, as nominally similar samples can expose different facets.

When the electrode is prepared by mechanical polishing, the defined fingerprint features vanish, which hinders the electrochemical characterization of the electrode based on cycling in the fingerprint region alone (Figure 2b).[19,20] However, the surface atomic structure can be elucidated by Pb-UPD, which reveals a preferential Cu(100) texture for the electrochemically and mechanically polished surface based on a very good agreement of the Pb monolayer deposition peak on both polycrystalline surfaces with the Cu(100) single crystal (Figure 2d). While the flat surface prepared by electropolishing also shows good agreement based on the stripping peak, this is not true for the surface prepared by mechanical polishing. We speculate that this lower reversibility of the process is linked to the rougher surface created by mechanical polishing (roughness factor of 2.6 for the mechanically polished sample and 1.0 for the electropolished sample such as described in detail in the Supporting Information) as Pb-UPD has been shown to be compromised on rough surface structures as a result of their porous morphology.[18]

After the mechanical polishing step on the rough SiC abrasive paper, it was investigated if the OH adsorption and desorption peaks can be recovered by subsequent electropolishing. However, even after repeated electropolishing at 2 V vs Cu in 66% phosphoric acid, the fingerprint CV shows no defined OH features (Figure S5). This result indicates that the electrode history significantly influences the observed adsorption features, and a simple electropolishing step cannot reset the electrode surface structure. Potentially the electrode needs to be polished with finer diamond or alumina paste and subsequently electropolished and/or annealed to reset the electrode. Additional research is necessary to elucidate the influence of electrode history on the adsorption features and reactivity and how to reset the electrode surface. We emphasize that if an electrode is reused for several experiments, then the surface structure should be checked for each experiment.

To evaluate whether the surface atomic structure of Cu-based catalysts can be probed before and after reaction, the influence of Pb on the electrochemical response of the Cu single crystals was investigated. Thereby, the steady-state cyclic voltammograms in Pb free solutions were compared to the steady state Pb-UPD voltammograms (Figures 1a−c). Especially for Cu(111), it becomes apparent that Cu does not undergo surface oxidation in the studied potential range in Pb containing solution even after the Pb stripping peak has been completed. This observation is surprising, as Pb ions in solution are not expected to inhibit the surface oxidation process. It is therefore likely that the Cu surface undergoes an irreversible change during the UPD process, which makes Cu more noble. A similar reduction in oxophilicity has also been observed in the literature for compressively strained Cu−Ag surface alloys where even a small fraction of Ag (~3 atomic %) was sufficient to alter the electrochemical characteristics of Cu.[41] Therefore, we expect an incorporation of Pb atoms into the Cu surface is likely to have a similar effect as Pb is also larger than Cu (similar to Ag). The Pb compresses the neighboring Cu atoms leading to a larger orbital overlap, which broadens the d-band of Cu. To maintain a constant filling, the d-band of Cu moves down which makes Cu less reactive (less oxophilic).[42]

To investigate this hypothesis, Cu(111) was held at 0.5 V vs RHE after Pb-UPD, and the crystal was then analyzed with X-ray photoelectron spectroscopy (XPS) and low energy ion

https://doi.org/10.1021/acs.langmuir.1c02830
Langmuir 2022, 38, 1514−1521

scattering (LEIS) (Figures 3a–c and Figure S6) after rinsing the sample thoroughly with Milli-Q water.

With both techniques, a significant amount of Pb was detectable on Cu with a near surface composition of ∼4% based on XPS. The residual amount of lead results from the irreversible incorporation of Pb into Cu during UPD as Pb does not galvanically exchange with Cu, and Pb is not expected to deposit onto Cu at open circuit voltage. This result is also supported by an earlier STM study that showed irreversible alloy formation of Cu and Pb upon UPD.[31] The formation of a surface alloy is an interesting observation as it shows that not only overlayers, but also surface alloys, can be synthesized *in situ* via underpotential deposition, which opens a new route of synthesizing this material class. This approach should be investigated in more detail in the future. However, this irreversible surface alloy formation also limits the applicability of Pb-UPD as a probe for the surface atomic structure of Cu-based catalysts to an analysis after the reaction.

To illustrate the potential of our developed method, we performed Pb-UPD after a 1 h CO reduction experiment at −0.7 V vs RHE (close to where a maximum in the ethylene partial current density for CO reduction on a polycrystalline Cu sample has been observed[18]). The investigated sample was a 200 nm sputtered film on a glassy carbon substrate that is nominally identical with the film investigated in Figure 2a. Compared to the Pb-UPD experiment on the sample before the reaction (Figure 2a), the underpotential deposition peak after CO reduction shifts from 0.354 V vs RHE to 0.322 V vs RHE, indicating a potential reconstruction of the sputtered Cu thin film (Figure S7). It should be stressed that the experiment was performed in a one-compartment cell with a graphite anode. Future experiments should be performed in a two-compartment cell with a membrane to separate anode and cathode. Additionally, these experiments should be combined with online product detection to directly correlate changes in the surface atomic structure to changes in the catalyst activity.

CONCLUSIONS

In summary, we successfully performed Pb-UPD on the three low index Cu single crystals under alkaline conditions and discussed the influence of specifically adsorbed hydroxide ions on the monolayer deposition and stripping of Pb. Using XPS and LEIS, we demonstrated that Cu and Pb form a surface alloy, which substantially alters the oxophilicity of Cu. This shows that UPD not only is a viable method to synthesize defined overlayer structures but also can be used for the *in situ* synthesis of surface alloys, which potentially can be viable catalysts for various reactions.[24,43] We then applied this knowledge to successfully probe the surface atomic structure of polycrystalline electrodes under alkaline conditions based on the established benchmark CVs of Pb-UPD on the Cu single crystals. Finally, we performed Pb-UPD on a 200 nm Cu thin film after 1 h CO reduction at −0.7 V vs RHE, which indicates a potential reconstruction of the sputtered thin film. We expect that this approach will facilitate the investigation of restructuring processes during electrochemical CO reduction in alkaline media as a post reaction UPD can be performed in the cell designs generally used for electrochemical CO reduction. Furthermore, we believe that underpotential deposition can be of general importance to characterize transition-metal-based electrodes as many catalysts are unstable under open circuit potential which compromises *ex situ* characterization techniques.[44] Beyond monometallic systems, the work function dependence of underpotential deposition can also be viable to determine the surface composition of alloys which can suffer from segregation induced by adsorption processes or the dissolution of one alloy component.[45−47]

ASSOCIATED CONTENT

Supporting Information

The Supporting Information is available free of charge at https://pubs.acs.org/doi/10.1021/acs.langmuir.1c02830.

Cyclic voltammograms in the fingerprint region of the three single crystals and the sputtered Cu thin film, a correlation of the amount of adsorbed hydroxide and the difference in expected and measured UPD shift, fingerprint CVs of the mechanically polished Cu stub after repeated electropolishing, an X-ray diffractogram of the sputtered Cu thin film, XPS survey scan of Cu(111) after Pb-UPD and Pb-UPD of the sputtered Cu thin film after 1 h CO reduction (PDF)

AUTHOR INFORMATION

Corresponding Author

Jakob Kibsgaard − *SurfCat Section for Surface Physics and Catalysis, Department of Physics, Technical University of Denmark, 2800 Kgs Lyngby, Denmark;* orcid.org/0000-0002-9219-816X; Email: jkib@fysik.dtu.dk

Authors

Degenhart Hochfilzer − *SurfCat Section for Surface Physics and Catalysis, Department of Physics, Technical University of Denmark, 2800 Kgs Lyngby, Denmark;* orcid.org/0000-0003-3654-909X

Aarti Tiwari − *SurfCat Section for Surface Physics and Catalysis, Department of Physics, Technical University of Denmark, 2800 Kgs Lyngby, Denmark;* Present Address: Department of Interface Science, Fritz-Haber Institute of the Max-Planck Society, 14195 Berlin, Germany

Ezra L. Clark − *SurfCat Section for Surface Physics and Catalysis, Department of Physics, Technical University of Denmark, 2800 Kgs Lyngby, Denmark*

Anton Simon Bjørnlund − *SurfCat Section for Surface Physics and Catalysis, Department of Physics, Technical University of Denmark, 2800 Kgs Lyngby, Denmark*

Thomas Maagaard − *SurfCat Section for Surface Physics and Catalysis, Department of Physics, Technical University of Denmark, 2800 Kgs Lyngby, Denmark;* orcid.org/0000-0002-2306-1506

Sebastian Horch − *SurfCat Section for Surface Physics and Catalysis, Department of Physics, Technical University of Denmark, 2800 Kgs Lyngby, Denmark;* Present Address: Department of Engineering Technology and Didactics, Technical University of Denmark, 2750 Ballerup, Denmark; orcid.org/0000-0001-7601-9224

Brian Seger − *SurfCat Section for Surface Physics and Catalysis, Department of Physics, Technical University of Denmark, 2800 Kgs Lyngby, Denmark;* orcid.org/0000-0002-0036-095X

Ib Chorkendorff − *SurfCat Section for Surface Physics and Catalysis, Department of Physics, Technical University of Denmark, 2800 Kgs Lyngby, Denmark;* orcid.org/0000-0003-2738-0325

Complete contact information is available at:
https://pubs.acs.org/10.1021/acs.langmuir.1c02830

Notes

The authors declare no competing financial interest.

■ ACKNOWLEDGMENTS

This work was supported by the Villum Foundation V-SUSTAIN Grant 9455 "The Villum Center for the Science of Sustainable Fuels and Chemicals", funding from the European Union's Horizon 2020 research and innovation programme under grant agreement no. 85144 (SELECT-CO_2) and funding from the European Union's Horizon 2020 research and innovation programme under Marie Sklodowska-Curie Grant Agreement 713683.

■ REFERENCES

(1) Rosca, V.; Duca, M.; de Groot, M. T.; Koper, M. T. M. Nitrogen cycle electrocatalysis. *Chem. Rev.* **2009**, *109* (6), 2209−2244.
(2) Kuhl, K. P.; Cave, E. R.; Abram, D. N.; Jaramillo, T. F. New insights into the electrochemical reduction of carbon dioxide on metallic copper surfaces. *Energy Environ. Sci.* **2012**, *5* (5), 7050.
(3) Bertheussen, E.; Hogg, T. V.; Abghoui, Y.; Engstfeld, A. K.; Chorkendorff, I.; Stephens, I. E. L. Electroreduction of CO on Polycrystalline Copper at Low Overpotentials. *ACS Energy Lett.* **2018**, *3* (3), 634−640.
(4) Hori, Y.; Murata, A.; Takahashi, R.; Suzuki, S. Enhanced formation of ethylene and alcohols at ambient temperature and pressure in electrochemical reduction of carbon dioxide at a copper electrode. *J. Chem. Soc., Chem. Commun.* **1988**, No. 1, 17.
(5) Bertheussen, E.; Verdaguer-Casadevall, A.; Ravasio, D.; Montoya, J. H.; Trimarco, D. B.; Roy, C.; Meier, S.; Wendland, J.; Nørskov, J. K.; Stephens, I. E. L.; Chorkendorff, I. Acetaldehyde as an Intermediate in the Electroreduction of Carbon Monoxide to Ethanol on Oxide-Derived Copper. *Angew. Chem.* **2016**, *128* (4), 1472−1476.
(6) Nitopi, S.; Bertheussen, E.; Scott, S. B.; Liu, X.; Engstfeld, A. K.; Horch, S.; Seger, B.; Stephens, I. E. L.; Chan, K.; Hahn, C.; Nørskov, J. K.; Jaramillo, T. F.; Chorkendorff, I. Progress and Perspectives of Electrochemical CO_2 Reduction on Copper in Aqueous Electrolyte. *Chem. Rev.* **2019**, *119* (12), 7610−7672.
(7) Chan, K. A few basic concepts in electrochemical carbon dioxide reduction. *Nat. Commun.* **2020**, *11* (1), 5954.
(8) Goodpaster, J. D.; Bell, A. T.; Head-Gordon, M. Identification of Possible Pathways for C-C Bond Formation during Electrochemical Reduction of CO_2: New Theoretical Insights from an Improved Electrochemical Model. *J. Phys. Chem. Lett.* **2016**, *7* (8), 1471−1477.
(9) Hori, Y.; Takahashi, I.; Koga, O.; Hoshi, N. Selective Formation of C2 Compounds from Electrochemical Reduction of CO 2 at a Series of Copper Single Crystal Electrodes. *J. Phys. Chem. B* **2002**, *106* (1), 15−17.
(10) Liu, X.; Schlexer, P.; Xiao, J.; Ji, Y.; Wang, L.; Sandberg, R. B.; Tang, M.; Brown, K. S.; Peng, H.; Ringe, S.; Hahn, C.; Jaramillo, T. F.; Nørskov, J. K.; Chan, K. pH effects on the electrochemical reduction of CO_2. towards C2 products on stepped copper. *Nat. Commun.* **2019**, *10* (1), 32.
(11) Schouten, K. J. P.; Kwon, Y.; van der Ham, C. J. M.; Qin, Z.; Koper, M. T. M. A new mechanism for the selectivity to C1 and C2 species in the electrochemical reduction of carbon dioxide on copper electrodes. *Chem. Sci.* **2011**, *2* (10), 1902.
(12) Schouten, K. J. P.; Pérez Gallent, E.; Koper, M. T. M. Structure Sensitivity of the Electrochemical Reduction of Carbon Monoxide on Copper Single Crystals. *ACS Catal.* **2013**, *3* (6), 1292−1295.
(13) Schouten, K. J. P.; Qin, Z.; Pérez Gallent, E.; Koper, M. T. M. Two pathways for the formation of ethylene in CO reduction on single-crystal copper electrodes. *J. Am. Chem. Soc.* **2012**, *134* (24), 9864−9867.
(14) Kim, Y.-G.; Baricuatro, J. H.; Javier, A.; Gregoire, J. M.; Soriaga, M. P. The evolution of the polycrystalline copper surface, first to Cu111. and then to Cu(100), at a fixed CO□RR potential: a study by operando EC-STM. *Langmuir* **2014**, *30* (50), 15053−15056.
(15) Scott, S. B.; Hogg, T. V.; Landers, A. T.; Maagaard, T.; Bertheussen, E.; Lin, J. C.; Davis, R. C.; Beeman, J. W.; Higgins, D.; Drisdell, W. S.; Hahn, C.; Mehta, A.; Seger, B.; Jaramillo, T. F.; Chorkendorff, I. Absence of Oxidized Phases in Cu under CO Reduction Conditions. *ACS Energy Lett.* **2019**, *4* (3), 803−804.
(16) Hochfilzer, D.; Sørensen, J. E.; Clark, E. L.; Scott, S. B.; Chorkendorff, I.; Kibsgaard, J. The Importance of Potential Control for Accurate Studies of Electrochemical CO Reduction. *ACS Energy Lett.* **2021**, *6* (5), 1879−1885.
(17) Tiwari, A.; Heenen, H. H.; Bjørnlund, A. S.; Maagaard, T.; Cho, E.; Chorkendorff, I.; Kristoffersen, H. H.; Chan, K.; Horch, S. Fingerprint Voltammograms of Copper Single Crystals under Alkaline Conditions: A Fundamental Mechanistic Analysis. *J. Phys. Chem. Lett.* **2020**, *11* (4), 1450−1455.
(18) Wang, L.; Nitopi, S.; Wong, A. B.; Snider, J. L.; Nielander, A. C.; Morales-Guio, C. G.; Orazov, M.; Higgins, D. C.; Hahn, C.; Jaramillo, T. F. Electrochemically converting carbon monoxide to liquid fuels by directing selectivity with electrode surface area. *Nat. Catal* **2019**, *2* (8), 702−708.
(19) Scott, S. B.; Engstfeld, A. K.; Jusys, Z.; Hochfilzer, D.; Knøsgaard, N.; Trimarco, D. B.; Vesborg, P. C. K.; Behm, R. J.; Chorkendorff, I. Anodic molecular hydrogen formation on Ru and Cu electrodes. *Catal. Sci. Technol.* **2020**, *10* (20), 6870−6878.
(20) Engstfeld, A. K.; Maagaard, T.; Horch, S.; Chorkendorff, I.; Stephens, I. E. L. Polycrystalline and Single-Crystal Cu Electrodes: Influence of Experimental Conditions on the Electrochemical Properties in Alkaline Media. *Chem. - Eur. J.* **2018**, *24* (67), 17743−17755.
(21) Tiwari, A.; Heenen, H. H.; Bjørnlund, A. S.; Hochfilzer, D.; Chan, K.; Horch, S. Electrochemical Oxidation of CO on Cu Single Crystals under Alkaline Conditions. *ACS Energy Lett.* **2020**, *5* (11), 3437−3442.
(22) Stephens, I. E. L.; Bondarenko, A. S.; Perez-Alonso, F. J.; Calle-Vallejo, F.; Bech, L.; Johansson, T. P.; Jepsen, A. K.; Frydendal, R.; Knudsen, B. P.; Rossmeisl, J.; Chorkendorff, I. Tuning the activity of Pt111. for oxygen electroreduction by subsurface alloying. *J. Am. Chem. Soc.* **2011**, *133* (14), 5485−5491.
(23) Mezzavilla, S.; Horch, S.; Stephens, I. E. L.; Seger, B.; Chorkendorff, I. Structure Sensitivity in the Electrocatalytic Reduction of CO_2 with Gold Catalysts. *Angew. Chem. Int. Ed.* **2019**, *58* (12), 3774−3778.
(24) Kim, C.; Möller, T.; Schmidt, J.; Thomas, A.; Strasser, P. Suppression of Competing Reaction Channels by Pb Adatom Decoration of Catalytically Active Cu Surfaces During CO 2 Electroreduction. *ACS Catal.* **2019**, *9* (2), 1482−1488.
(25) Kolb, D. M.; Przasnyski, M.; Gerischer, H. Underpotential deposition of metals and work function differences. *Journal of Electroanalytical Chemistry and Interfacial Electrochemistry* **1974**, *54* (1), 25−38.
(26) Herrero, E.; Buller, L. J.; Abruña, H. D. Underpotential deposition at single crystal surfaces of Au, Pt, Ag and other materials. *Chem. Rev.* **2001**, *101* (7), 1897−1930.
(27) Mayet, N.; Servat, K.; Kokoh, K. B.; Napporn, T. W. Probing the Surface of Noble Metals Electrochemically by Underpotential Deposition of Transition Metals. *Surfaces* **2019**, *2* (2), 257−276.
(28) Sebastián-Pascual, P.; Escudero-Escribano, M. Surface characterization of copper electrocatalysts by lead underpotential deposition. *J. Electroanal. Chem.* **2021**, *896*, 115446.
(29) Raaijman, S. J.; Arulmozhi, N.; Koper, M. T. M. Morphological Stability of Copper Surfaces under Reducing Conditions. *ACS Appl. Mater. Interfaces* **2021**, *13*, 48730.
(30) Roberts, F. S.; Kuhl, K. P.; Nilsson, A. High Selectivity for Ethylene from Carbon Dioxide Reduction over Copper Nanocube Electrocatalysts. *Angew. Chem.* **2015**, *127* (17), 5268−5271.

(31) Moffat, T. P. Oxidative Chloride Adsorption and Lead Upd on Cu(100): Investigations into Surfactant-Assisted Epitaxial Growth. *J. Phys. Chem. B* **1998**, *102* (49), 10020−10026.
(32) Engbæk, J.; Lytken, O.; Nielsen, J. H.; Chorkendorff, I. CO dissociation on Ni: The effect of steps and of nickel carbonyl. *Surf. Sci.* **2008**, *602* (3), 733−743.
(33) Hörmann, N. G.; Andreussi, O.; Marzari, N. Grand canonical simulations of electrochemical interfaces in implicit solvation models. *J. Chem. Phys.* **2019**, *150* (4), 41730.
(34) Brisard, G. M.; Zenati, E.; Gasteiger, H. A.; Markovic, N.; Ross, P. N. Underpotential Deposition of Lead on Copper(111): A Study Using a Single-Crystal Rotating Ring Disk Electrode and ex Situ Low-Energy Electron Diffraction and Scanning tunneling Microscopy. *Langmuir: the ACS journal of surfaces and colloids* **1995**, *11* (6), 2221−2230.
(35) Brisard, G. M.; Zenati, E.; Gasteiger, H. A.; Marković, N. M.; Ross, P. N. Underpotential Deposition of Lead on Cu100. in the Presence of Chloride: Ex-Situ Low-Energy Electron Diffraction, Auger Electron Spectroscopy, and Electrochemical Studies. *Langmuir: the ACS journal of surfaces and colloids* **1997**, *13* (8), 2390−2397.
(36) Nagl, C.; Haller, O.; Platzgummer, E.; Schmid, M.; Varga, P. Submonolayer growth of Pb on Cu(111): surface alloying and de-alloying. *Surf. Sci.* **1994**, *321* (3), 237−248.
(37) Nagl, C.; Platzgummer, E.; Haller, O.; Schmid, M.; Varga, P. Surface alloying and superstructures of Pb on Cu(100). *Surf. Sci.* **1995**, *331*−*333*, 831−837.
(38) de Beauvais, C.; Girard, Y.; Pérard, C.; Croset, B.; Mutaftschiev, B. Surface alloying of Pb on Cu(111): a TEAS study. *Surf. Sci.* **1996**, *367* (2), 129−134.
(39) Gauthier, Y.; Moritz, W.; Hösler, W. Surface alloy in the c(4 × 4) phase of Pb on Cu(100). *Surf. Sci.* **1996**, *345* (1−2), 53−63.
(40) Krastev, E. T.; Voice, L. D.; Tobin, R. G. Surface morphology and electric conductivity of epitaxial Cu100. films grown on H-terminated Si(100). *J. Appl. Phys.* **1996**, *79* (9), 6865−6871.
(41) Clark, E. L.; Hahn, C.; Jaramillo, T. F.; Bell, A. T. Electrochemical CO_2 Reduction over Compressively Strained CuAg Surface Alloys with Enhanced Multi-Carbon Oxygenate Selectivity. *J. Am. Chem. Soc.* **2017**, *139* (44), 15848−15857.
(42) Hammer, B.; Norskov, J. K. Why gold is the noblest of all the metals. *Nature* **1995**, *376* (6537), 238−240.
(43) Sun, J.; Lao, X.; Yang, M.; Fu, A.; Chen, J.; Pang, M.; Gao, F.; Guo, P. Alloyed Palladium-Lead Nanosheet Assemblies for Electrocatalytic Ethanol Oxidation. *Langmuir* **2021**, *37*, 14930.
(44) Wang, Z.; Zheng, Y.-R.; Montoya, J.; Hochfilzer, D.; Cao, A.; Kibsgaard, J.; Chorkendorff, I.; Nørskov, J. K. Origins of the Instability of Nonprecious Hydrogen Evolution Reaction Catalysts at Open-Circuit Potential. *ACS Energy Lett.* **2021**, *6* (6), 2268−2274.
(45) Schalenbach, M.; Speck, F. D.; Ledendecker, M.; Kasian, O.; Goehl, D.; Mingers, A. M.; Breitbach, B.; Springer, H.; Cherevko, S.; Mayrhofer, K. J. Nickel-molybdenum alloy catalysts for the hydrogen evolution reaction: Activity and stability revised. *Electrochim. Acta* **2018**, *259*, 1154−1161.
(46) Nerlov, J.; Chorkendorff, I. Methanol Synthesis from CO_2, CO, and H2over Cu100. and Ni/Cu(100). *J. Catal.* **1999**, *181* (2), 271−279.
(47) Tao, F.; Grass, M. E.; Zhang, Y.; Butcher, D. R.; Renzas, J. R.; Liu, Z.; Chung, J. Y.; Mun, B. S.; Salmeron, M.; Somorjai, G. A. Reaction-driven restructuring of Rh-Pd and Pt-Pd core-shell nanoparticles. *Science (New York, N. Y.)* **2008**, *322* (5903), 932−934.

https://doi.org/10.1021/acs.langmuir.1c02830
Langmuir 2022, 38, 1514−1521